Effect of a high angle grain boundary on deformation behavior of Al nanopillars

Youbin Kim,[a] Subin Lee,[b] Jong Bae Jeon,[b,c] Yong-Jae Kim,[a] Byeong-Joo Lee,[b] Sang Ho Oh[b,*] and Seung Min Han[a,*]

[a]Graduate School of EEWS, Korea Advanced Institute of Science and Technology, Daejeon 305-701, Republic of Korea
[b]Department of Materials Science and Engineering, Pohang University of Science and Technology (POSTECH), Pohang 790-784, Republic of Korea
[c]Functional Components and Materials R&D Group, Korea Institute of Industrial Technology, Busan 618-230, Republic of Korea

The effect of inclusion of a grain boundary in nanopillar was studied using Al bicrystal with [343]/[13$\overline{17}$14] orientation. Ex situ compression results showed higher strengths in bicrystal pillars than in single crystal pillars, which is explained with respect to the reduced single-armed source length that was confirmed in the in situ TEM tests. Molecular dynamics simulations indicated that the grain boundary can assist in dislocation nucleations without resulting in dislocation pile-up at the boundary.
© 2015 Acta Materialia Inc. Published by Elsevier Ltd. All rights reserved.

Understanding the strengthening effects of grain boundaries in bulk metals and alloys has been of importance and extensively studied over the past decades [1–6]. In the case of polycrystalline bulk metals, the strength is known to increase as the grain size is reduced since dislocations are piled-up at each grain boundary and thus require a higher stress to overcome the resistance from the boundary before being transmitted across the boundary. This is the basis for the well-known Hall–Petch relation, $\sigma \propto kd^{-1/2}$, where k and d are the strengthening coefficient and the grain size, respectively [7–8].

A different type of size-dependent strengthening has been studied and is well-documented for the case of single crystal metal nanopillars. As the external dimension is reduced to submicrons in diameter, the metal nanopillars are known to exhibit increasing the strength as well as plastic flow being more stochastic in nature [9–13]. Rather than Taylor hardening, plasticity in metal nanopillars can occur via surface nucleations in the absence of defects within the small volume of the nanopillar [14,15], or single-armed source operations can lead to increased flow stresses during plastic deformation [16,17]. This size dependency of flow stresses can be characterized by the power-law relation, $\sigma_{ys} \propto d^{-n}$, where d is the diameter of nanopillar and n is the power-law exponent.

An interesting question arises as to what will be the role of a single high angle grain boundary if it is inserted in the middle of a nanopillar such as in the case of a bicrystal. In the traditional sense, a grain boundary is expected to cause strengthening as a result of Hall–Petch effect as described above. However, a grain boundary in bicrystal nanopillar can be regarded as an additional interface from which dislocation nucleations can occur that could potentially cause weakening as a consequence of easier dislocation nucleations [18]. In the case of a built-in single-armed source governing the deformation of a nanopillar, the grain boundary, similar to the free surface, can also act as a geometrical constraint limiting the available source size, resulting in higher strengths. The dislocations emitted from the source can first be blocked by the grain boundary for further propagation but potentially be guided to escape through the nearby free surface, thereby preventing any pile-up of dislocations at the grain boundary. Therefore, the role of grain boundary in a nanopillar may not simply be accounted for by the Hall–Petch type strengthening [19].

Up to date, there are few experimental studies for the deformation of bicrystal nanopillars available. The first is the study by Ng et al. [20] for Al single and bicrystal pillars with [6$\overline{4}$1]/[4$\overline{1}$$\overline{2}$] orientation and pillar sizes in the range of 2–6 μm in diameter. The authors proposed that the grain boundary may cause dislocation storage, based on their observation of the bicrystal pillars displaying a higher strength and more homogeneous deformation than in

* Corresponding authors; e-mail addresses: shoh@postech.ac.kr; smhan01@kaist.ac.kr

2   Y. Kim et al. / Scripta Materialia xxx (2015) xxx–xxx

single crystals. A transmission electron microscopy (TEM) image directly showing a high density of dislocations in pile-up array at the grain boundary was used to support their idea. In contrast, an independent study conducted by Kunz et al. [21] on Al bicrystal with the [1 0 4]/[1 2 6] orientation for diameters ranging from 400 nm to 2 μm claimed a different role of grain boundary: a sink for absorbing dislocations. The authors indicated that the strengths of bicrystal nanopillars were similar to those of single crystal pillars, while the bicrystal nanopillars exhibited lower hardenability and larger average strain bursts during plastic flow. The TEM images of deformed bicrystal nanopillars showing the lack of dislocation build-up near the grain boundary provided an experimental support to claim that the grain boundary may act as a dislocation sink. The discrepancy between the results is likely due to the different nature of grain boundary and also to the different size ranges studied. For example, dislocation starvation through dislocation-boundary interaction can occur in small samples while large samples harden through dislocation–dislocation interaction [22].

In this study, we systematically studied the effect of inclusion of single high angle grain boundary in Al bicrystal nanopillar with the orientation of [3 4 3]/[13 $\overline{17}$ 14] to determine the overall mechanical response at the nanoscale using ex situ and in situ TEM compression tests and molecular dynamic (MD) simulations.
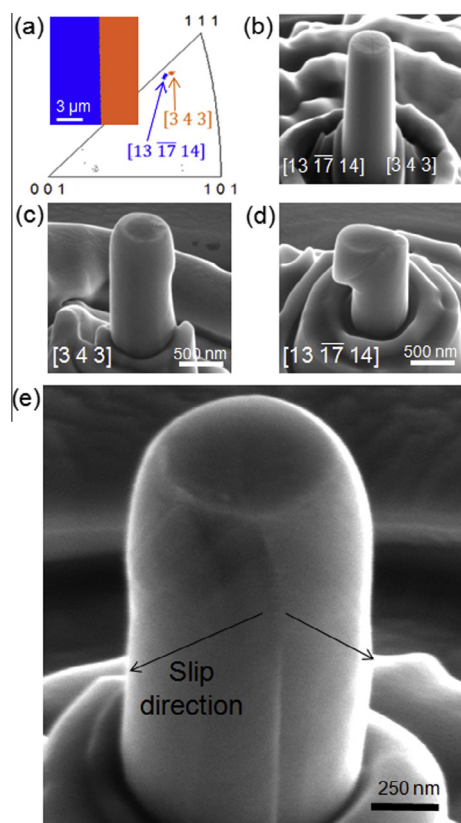

Figure 1. (a) Grain orientation map of Al bicrystal obtained by EBSD showing the out-of-plane orientations of [3 4 3] and [13$\overline{17}$14]. SEM images of (b) as-fabricated bicrystal nanopillar and single crystal nanopillars after deformation for (c) [3 4 3] and (d) [13$\overline{17}$14] orientations. (e) High-magnification SEM image for deformed bicrystal pillar showing grain boundary and slip traces.

The Al bulk sample with a single high angle grain boundary was fabricated with co-solidification using two seeds, and the grain orientation was confirmed by electron backscatter diffraction (EBSD) in FEI Quanta SEM (Fig. 1(a)). The compression directions for adjacent grains are [3 4 3] and [13 $\overline{17}$ 14], respectively, with a misorientation angle of 60.9° around [17 19 10]. In order to fabricate pillars along the grain boundary, a gentle diluted hydrofluoric acid (HF) etch was used to reveal the boundary on the surface of the specimen. The Quanta 3D FEG focused ion beam (FIB) was utilized to fabricate the nanopillars with a fixed diameter-to-height ratio of 1:3 to avoid buckling of the sample during compression. A pedestal of 30 μm in outer diameter and 10 μm in inner diameter was made first, and the pedestal was reduced down to the final pillar dimensions using finer ion beam currents. The pillar diameter was chosen to vary over a wide range between 200 nm and 2 μm. All bicrystal pillars were fabricated with the grain boundary positioned in the middle, and thus the grain boundary is then oriented perpendicular to the top surface as shown in Figs. 1(b), (e) and 3. Single crystal pillars were also made on both sides of the grain boundaries to obtain [3 4 3] and [13 $\overline{17}$ 14] oriented pillars.

The fabricated nanopillars were tested in compression using the Hysitron Tbi-750 (Minneapolis, MN) nanoindentation system with a 10 μm diameter flat-ended diamond cube corner tip. All pillars were compressed in a displacement control feedback mode (DC mode) using the Hysitron quasistatic indentation transducer with a nominal engineering strain rate of 0.002 s^{-1}. More than 20 pillars were fabricated and tested from both single and bicrystal sections of the specimen, and all pillars were tested to a total strain of larger than 15%. For the in situ TEM compression testing, bicrystal nanopillar with a diameter of 200 nm was fabricated using FIB and fixed on a Cu support grid. A nanoindentation TEM holder (Nanofactory) equipped with a diamond flat punch was used for the compression test in TEM. The experiments were carried out in a field-emission TEM operated at 200 kV (JEM-2100F, JEOL), and real-time movies were recorded with a charge coupled device camera (ORIUS 200D, Gatan). The bicrystal pillar was compressed to the total strain of ~2% at a low strain rate, ~1 nm s^{-1}.

MD simulation was performed on a bicrystal nanopillar with the diameter of 10–30 nm in the same orientation as the specimen used for experiments without any initial dislocations or any pinning points. Two interatomic potential models for Al of embedded atom method (EAM) [23] and the second nearest-neighbor modified embedded atom method (2NN-MEAM) [24] were employed to guarantee the reliability of the results. Periodic boundary condition was applied along the longitudinal compression axis. Dynamics with isobaric-isothermal (NPT) ensemble were carried out for 0.5 ns for thermal equilibration. Compression tests were then conducted with canonical (NVT) ensemble at 300 K at a constant strain rate of 5 × 10^8 s^{-1}.

The SEM images of the deformed nanopillars shown in Figure 1(c–e) indicate that the bicrystal nanopillar deformed homogeneously while the single crystal nanopillar resulted in inhomogeneous deformation due to strain localization near the slip steps. The slip system with the maximum Schmid factors for the [3 4 3] and [13 $\overline{17}$ 14] orientations are: both ($\overline{1}$ 1 1) [1 1 0] and (1 $\overline{1}$ 1) [0 1 1] slip systems for the [3 4 3] oriented grain, which is 0.336, and ($\overline{1}$ 1 1) [0 $\overline{1}$ 1] slip system for [13 $\overline{17}$ 14] oriented grain, which is 0.31. Therefore, the expected angle between the load